A Time-Domain Impedance Element for FEA of Axisymmetric Exterior Structural Acoustics

L. F. Kallivokas

J. Bielak

Computational Mechanics Laboratory,
Department of Civil Engineering,
Carnegie Mellon University,
Pittsburgh, PA 15213

A finite element (FE)-based procedure is presented for the solution directly in the time-domain of transient problems involving axisymmetric three-dimensional structures submerged in an infinite acoustic fluid. The central component of the procedure is a novel impedance element that is used to render the computational domain finite. The element is local in both time and space, and is completely defined by a pair of stiffness and damping matrices. It is shown that the exterior structural acoustics problem can be solved accurately and efficiently by using the same tools as those used for interior problems. The method is illustrated with numerical results for a submerged shell.

Introduction

The exterior structural acoustics problem typically involves the determination of the displacement and/or stress field of a structure submerged in an infinite acoustic fluid and the pressure field within the surrounding fluid, given an incident pressure field or radiation loading acting on the structure. A primary difficulty associated with the study of this problem is the need to deal with the infinite fluid, that is, the modeling of the Sommerfeld radiation condition. To date, frequency-domain approaches are predominant (see Jeans and Mathews (1990) for a partial list), due, at least in part, to the relative ease of incorporating the radiation condition in the frequency domain as opposed to the time domain. Direct time-domain approaches are, however, often needed as the only viable means for tackling problems that involve inelastic behavior, or structural or noise control, or optimum structural design. One direct approach is to truncate the infinite domain by introducing an artificial boundary within the fluid and to specify a boundary condition that will satisfy approximately the radiation condition. An inherent difficulty with such absorbing boundary methodologies is the assurance of stability of the approximate conditions and validity for late time (low frequency), since these conditions are usually constructed using high frequency approximations. A classical representation of an early time (high frequency) approximation is the well-known plane wave approximation (PWA), first used by Mindlin and Bleich (1953). A late time (low frequency) virtual mass approximation was later developed by Chertock (1970), and in the 1970s Geers (1971, 1978), by combining the early and late time approaches, derived a doubly asymptotic approximation (DAA) that can be enforced directly on the surface of the structure. The price one pays for this benefit, however, is having to deal with a spatially nonlocal boundary, since, at each instant, DAAs couple the response at each point of the artificial boundary with that at every other point.

Absorbing boundaries that are local in both time and space, yet of a higher order of accuracy than the earlier PWA, have been proposed by several authors. A survey of various absorbing boundary treatments up to 1990 is given by Givoli (1991). Here we mention the well-known sequences of boundary conditions obtained by Engquist and Majda (1979) and Bayliss and Turkel (1980). A finite element scheme for solving the acoustic radiation problem using Bayliss and Turkel's second-order approximation has been implemented by Pinsky et al. (1992) and by Pinsky and Abboud (1990, 1991) for two- and three-dimensional problems, respectively, and has been illustrated for simple radiation problems; the nonsymmetric character of the boundary treatment in the latter references destroys the symmetry of the global equations.

Barry et al. (1988) have developed a family of approximate boundary conditions for the transient two-dimensional wave equation using ideas of geometrical optics. By giving it a viscoelastic interpretation, Kallivokas et al. (1991) were able to recast the second-order condition of Barry et al. (1988) into an equivalent form that can be represented completely, upon discretization, by a very simple impedance element on the boundary, local in time and space. The impedance element was recently (Kallivokas and Bielak, 1993) used to formulate the two-dimensional fluid-structure interaction problem; here we extend these ideas to three-dimensional axisymmetric problems. The practical significance of the novel element, which can be completely characterized by a pair of stiffness and damping symmetric matrices, is that it makes it possible, apparently for the first time, to solve accurately and efficiently exterior initial-value problems in three-dimensional axisymmetric structural acoustics, and other multiphase phenomena, with existing finite element software for interior problems. In order to obtain a symmetric formulation we use a variational formulation in terms of the displacement field and the velocity potential field introduced originally by Everstine (1981), for the structure and the fluid, respectively. We concentrate on the thin spherical elastic shell, using this canonical geometry as a benchmark since the

Contributed by the Technical Committee on Vibration and Sound for publication in the JOURNAL OF VIBRATIONS AND ACOUSTICS. Manuscript received May 1993. Associate Technical Editor: G. Koopman.

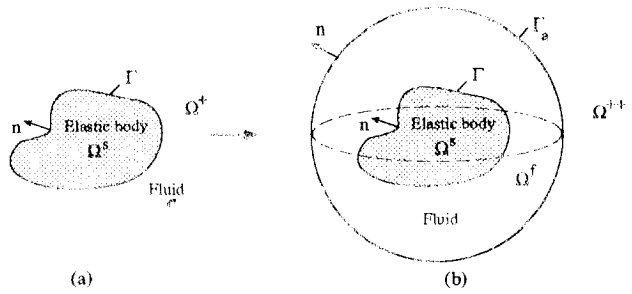

Fig. 1 (*a*) Model of fluid-structure interaction system; (*b*) reduced model with finite fluid region and absorbing boundary

corresponding transient scattering problem is amenable to exact solution. Arbitrary axisymmetric elastic structures can be analyzed similarly merely by modifying the expression for the strain energy in the variational principle. We present numerical results for a scattering problem for the homogeneous shell and for a limiting rigid scatterer using a finite-duration modified Ricker (1977) pulse as excitation.

1 Problem Description and Absorbing Boundaries

We discuss initially the treatment of the infinite acoustic fluid by assuming a general three-dimensional structure submerged in it; we subsequently particularize for the case of a submerged spherical shell. Suppose Ω^s represents the region occupied by the structure, Ω^+ the corresponding exterior region, and Γ their interface, as shown in Fig.1(*a*). We assume that the homogeneous, compressible, and inviscid fluid remains close to an equilibrium state with constant density and velocity. We also assume that there is an incident transient fluid motion given by a pressure p^0, where p^0 satisfies the wave equation with speed of sound c; the simple modifications needed to consider the corresponding radiation problem will be discussed later. Following Everstine (1981), we introduce the velocity potential function, ψ, through the following relationships:

$$\mathbf{v}^s = \nabla\psi, \quad \mathbf{v}^f = \nabla\psi - \frac{1}{\rho}\nabla\int_0^t p^0 dt, \quad P = -\rho\dot{\psi} + p^0, \quad (1)$$

where $\mathbf{v}^s$ and $\mathbf{v}^f$ are, respectively, the scattered and total velocity of the fluid, P denotes the total pressure, ρ is the density of the fluid, and ∇ and an overdot denote, respectively, vector gradient and derivative with respect to time. With this choice of ψ, $-\rho\dot{\psi}$ represents the scattered pressure. It can be shown that ψ satisfies the wave equation within Ω^+:

$$c^2\nabla^2\psi = \ddot{\psi}. \quad (2)$$

Since the scattered wave $-\rho\dot{\psi}$ must be outgoing, then ψ must satisfy a radiation condition at infinity. Rather than considering the structural acoustic scattering problem over the entire infinite domain $\mathcal{R}^3$ we introduce an artificial, smooth, convex boundary Γ_a in Ω^+ and pose an equivalent problem over the finite region $\Omega^s \cup \bar{\Omega}^f$, as shown in Fig. 1(*b*) in which Ω^f is the region occupied by the fluid, and $\bar{\Omega}^f$ is its closure (i.e., Ω^f and its boundaries Γ and Γ_a). Then on Γ_a, ψ will satisfy an exact nonlocal condition for the normal derivative, $\psi_n = \nabla\psi \cdot n$, where n is the unit outer normal to Γ_a, of the form:

$$\psi_n = \mathfrak{F}\left[\psi^t(\cdot,\cdot)\right]. \quad (3)$$

The right side of (3) denotes a functional of the values of $\psi(\xi, \zeta)$ for ξ ranging over Γ_a and ζ from 0 to t, with the notation ψ^t implying time histories for ψ. Hence, $\mathfrak{F}$ is the exact operator expressing the spatial and temporal non-locality on Γ_a. In other words, $\mathfrak{F}$ merely indicates that at a given instant t the motion at every point on the artificial boundary Γ_a is coupled with the time histories of all other points on Γ_a.

The idea then is to approximate $\mathfrak{F}$ so as to reduce the temporal non-locality. To this end, we formulate the following problem in the region Ω^{f+} exterior to Ω^f:

$$c^2\nabla^2 V(\mathbf{x},s;t) = s^2 V(\mathbf{x},s;t), \quad \mathbf{x} \in \Omega^{f+}, \quad (4a)$$

with

$$V(\mathbf{x},s;t) = \psi(\mathbf{x},t), \quad \mathbf{x} \in \Gamma_a, \quad (4b)$$

in which $\mathbf{x}$ denotes a position vector and s is the Laplace transform variable. Notice that in these and subsequent equations the use of a semicolon before t in the argument list of functions implies that t acts as a parameter. It can be shown that on Γ_a there holds:

$$\hat{\psi}_n(\mathbf{x},s) = \int_0^\infty e^{-st} V_n(\mathbf{x},s;t)dt = \hat{\mathfrak{F}}\left[\hat{\psi}(\cdot,s)\right](\mathbf{x},s), \quad (5)$$

in which a caret denotes Laplace transform. Therefore, if one could approximate V_n on Γ_a, one would find the desirable approximation for the exact operator $\mathfrak{F}$ on Γ_a. For this purpose consider next a high-frequency expansion for V of the form:

$$V(\mathbf{x},s;t) \sim e^{-\frac{s}{c}g(\mathbf{x})} \sum_{k=0}^{\infty}\left[\frac{c}{(s+\gamma)R}\right]^k A^{(k)}(\mathbf{x},t), \quad \mathbf{x} \in \bar{\Omega}^{f+}, \quad (6a)$$

in which $g(\mathbf{x})$ and $A^{(k)}(\mathbf{x}, t)$ as yet unknown functions that satisfy the following conditions on Γ_a:

$$g(\mathbf{x}) = 0, \quad A^{(0)}(\mathbf{x},t) = \psi(\mathbf{x},t), \quad A^{(k)}(\mathbf{x},t) = 0, \quad k \geq 1. \quad (6b)$$

In these equations, γ is an arbitrary nonnegative parameter whose value controls the amount of numerical damping introduced through the boundary Γ_a, and R is a characteristic length of the boundary Γ_a (e.g., in the case of a spherical boundary, R is the radius). Equations (6) ensure that V is outgoing and that (4*b*) is satisfied automatically for any functions g and $A^{(k)}$. By introducing (6) into (4*a*) and matching the coefficients of the various powers of s one obtains a set of recursive differential equations for the unknown functions g and $A^{(k)}$. From these equations it can be further shown that for a spherical absorbing boundary of radius R, g and the first two terms $A^{(0)}$ and $A^{(1)}$ satisfy the following relationships in Ω^{f+} for the axisymmetric case:

$$g = r - R, \quad A_r^{(0)} = -\frac{1}{r}A^{(0)}(r,\phi,t),$$

$$A_r^{(1)} = \frac{R}{2}\frac{1}{r^2\sin\phi}\left(A_\phi^{(0)}(r,\phi,t)\sin\phi\right)_\phi - \frac{1}{r}A^{(1)}(r,\phi,t), \quad (7)$$

in which (r, ϕ) denote spherical coordinates, with r being the radial coordinate and ϕ the polar angle along a meridian and subscripts denote partial derivatives; the problem is symmetric with respect to the azimuth.

Next, by making use of (6*a*), (6*b*), and taking (7) into consideration, (5) becomes:

$$\hat{\psi}_r(R,\phi,s) = -\frac{s}{c}\hat{A}^{(0)}(R,\phi,s) + \sum_{k=0}^{\infty}\left[\frac{c}{(s+\gamma)R}\right]^k \hat{A}_r^{(k)}(R,\phi,s), \quad \text{on } \Gamma_a. \quad (8)$$

Equation (8) can be used to obtain successive approximations in the Laplace transform domain for $\hat{\psi}_r$ by truncating the

series in (8); for example, the first approximation involves only the first term on the right-hand side of (8), the second approximation involves the first term on the right-hand side of (8) plus the first term of the series in (8), etc. We use (7) and (8) to obtain the first three approximations in the transform domain and subsequently invert the resulting expressions in the time-domain to obtain the following results:

$$\psi_r = -\frac{1}{c}\dot{\psi}, \tag{9a}$$

$$\psi_r = -\frac{1}{c}\dot{\psi} - \frac{1}{R}\psi, \tag{9b}$$

$$\dot{\psi}_r + \gamma\psi_r = -\frac{1}{c}\ddot{\psi} - \left(\frac{1}{R} + \frac{\gamma}{c}\right)\dot{\psi} + \frac{c}{2R^2\sin\phi} \times \left(\psi_\phi \sin\phi\right)_\phi - \frac{\gamma}{R}\psi, \tag{9c}$$

For the numerical examples considered herein, γ was set equal to c/R. For this particular value, (9c) reduces to the second-order condition derived by Bayliss and Turkel (1980). The first approximation is identical to the Mindlin and Bleich (1953) PWA approximation, while the second one coincides with the first order expression from Bayliss and Turkel (1980). We remark that the Laplace transform of (9c) differs from that of the exact absorbing boundary condition (3) by terms of order $(c/(Rs))^2$; hence the designation of second-order for the latter approximation.

Any one of Eqs. (9) can be used as an approximation to the right-hand side of (3). However, Eq. (9c) entails a smaller computational domain for the same level of numerical accuracy; it is hence preferable over (9a) and (9b) for numerical applications. This equation, however, has the disadvantage that it contains a linear combination of ψ_r and its time derivative, $\dot{\psi}_r$, rather than being expressed in terms of ψ_r by itself, as required in a variational formulation. This has the consequence of destroying the symmetry of the original problem (and perhaps also decreasing the accuracy of the numerical procedure) since (9c) requires that the derivative of ψ_r with respect to time be approximated numerically. In order to retain the symmetry, we introduce an additional degree of freedom on the boundary Γ_a, namely $\psi^{(1)}$ which allows condition (9c) to be replaced by the following equivalent system of two equations:

$$-\psi_r = \frac{1}{c}\dot{\psi} + \frac{1}{R}\psi - \frac{c}{2\gamma R^2}\left[\left(1-\eta^2\right)\psi_\eta^{(1)}\right]_\eta, \tag{10a}$$

$$\left[\left(1-\eta^2\right)\left(\psi_\eta^{(1)} - \psi_\eta\right)\right]_\eta = -\frac{1}{\gamma}\left[\left(1-\eta^2\right)\dot{\psi}_\eta^{(1)}\right]_\eta, \tag{10b}$$

where $\eta = \cos\phi$. Now (10a) has the desired form. Even though it contains one new variable and the introduction of this variable adds one new equation to the formulation, the set of Eqs. (10) can be readily incorporated into a variational formulation.

Thus, the structural acoustics problem, in its exact formulation, consists in solving the equations of elasto-dynamics for the displacement field within Ω^s and the wave Eq. (2) in Ω^f for the velocity potential field, under zero initial conditions, due to the incident pressure p^0. In addition, the traction and the normal velocity must be continuous across the interface Γ and ψ must satisfy the radiation condition (3). p^0 and its normal derivative enter into the formulation through the transition condition across Γ. For the approximate problem one replaces (3) by either (9a), (9b), or the two equations (10).

2 Variational Formulation

In order to derive a finite element approximation for the structural acoustics problem described in the preceding section it is desirable to have a variational formulation of the problem. In this section we develop a direct variational formulation for the particular case of a spherical shell, using Hamilton's principle as a point of departure. To this end, consider a spherical shell of thickness d and radius a referred to an (r, ϕ, θ) spherical coordinate system. We consider here only the axisymmetric case for which the component of motion along the direction of θ (meridional angle) vanishes. Let the radial and circumferential midsurface components be denoted by w and v, respectively. We use the thin shell theory as presented by Junger and Feit (1972). For this shell-fluid system, Hamilton's principle can be expressed as:

$$\delta\int_{t_1}^{t_2}\left(T_s + T_f - V_s - V_f\right)dt = -\int_{t_1}^{t_2}\left[-\int_\Gamma P\delta w dS + \int_\Gamma (u^f\cdot n)\delta P dS - \int_{\Gamma_a}(u^f\cdot n)\delta P dS\right]dt, \tag{11}$$

in which (Junger and Feit, 1972)

$$T_s = \pi\rho_s d\int_\Gamma (\dot{v}^2 + \dot{w}^2)dS, \tag{12a}$$

$$T_f = \frac{1}{2}\rho\int_{\Omega^f}\mathbf{v}^f\cdot\mathbf{v}^f d\Omega, \tag{12b}$$

$$V_s = \frac{\pi E d}{1-\nu^2}\frac{1}{a^2}\left\{\int_\Gamma\left[(v_\phi + w)^2 + (v\cot\phi + w)^2 + 2\nu(v_\phi + w)(v\cot\phi + w)\right]dS + \beta^2\int_\Gamma\left[(v_\phi - w_{\phi\phi})^2 + \cot^2\phi(v - w_\phi)^2 + 2\nu\cot\phi(v_\phi - w_{\phi\phi})(v - w_\phi)\right]dS\right\}, \tag{12c}$$

$$V_f = \frac{1}{2\rho c^2}\int_{\Omega^f}P^2 d\Omega. \tag{12d}$$

Here ρ_s, E, ν, are the mass density, Young's modulus, Poisson's ratio of the shell, $\beta^2 = d^2/12a^2$, t_1 and t_2 are two arbitrary instants, $\mathbf{u}^f$ is the displacement within the fluid ($\dot{\mathbf{u}}^f = \mathbf{v}^f$) and the surface differential dS is equal to $a^2\sin\phi d\phi$. Equation (11) is a statement of the condition that the sum of the variation of the Lagrangian must be equal to the negative of the virtual work done by external agents acting on each subsystem. T_s and T_f are the kinetic energy in the shell and fluid, respectively, V_s is the strain energy in the shell, and V_f the potential energy in the fluid. The first integral on the right is the virtual work done on the shell by the fluid pressure, while the second and third terms represent the corresponding work on the inner (Γ) and outer (Γ_a) boundaries of the fluid. If one substitutes (1), (12) and the exact boundary condition (3) on Γ_a into (11), after integration by parts, (11) reduces to the following form:

$$\int_{t_1}^{t_2}\left\{-2\pi\rho_s d\int_\Gamma(\ddot{v}\delta v + \ddot{w}\delta w)dS + \frac{\rho}{c^2}\int_{\Omega^f}\ddot{\psi}\delta\psi d\Omega - \frac{2\pi E d}{1-\nu^2}\frac{1}{a^2}\left\{\int_\Gamma\left[(v_\phi + w)(\delta v_\phi + \delta w) + (v\cot\phi + w) \times (\delta v\cot\phi + \delta w) + \nu(\delta v_\phi + \delta w)(v\cot\phi + w) + \nu(v_\phi + w)(\delta v\cot\phi + \delta w)\right]dS - \beta^2\int_\Gamma\left[(\delta v_\phi - \delta w_{\phi\phi})\right.\right.$$

$$\times(v_\phi - w_{\phi\phi}) + \cot^2\phi(\delta v - \delta w_\phi)(v - w_\phi)$$
$$+\nu\cot\phi(\delta v_\phi - \delta w_{\phi\phi})(v - w_\phi) + \nu\cot\phi(v_\phi - w_{\phi\phi})$$
$$\times(\delta v - \delta w_\phi)]dS\Big\} + \rho\int_{\Omega^f}\nabla\psi\cdot\nabla\delta\psi d\Omega + \rho\int_\Gamma \dot\psi\delta w dS$$
$$+\rho\int_\Gamma \dot w\delta\psi dS - \rho\int_{\Gamma_a}\mathfrak{F}[\psi]\delta\psi dS_a\Big)dt$$
$$= \int_{t_1}^{t_2}\Big(\int_\Gamma p^0\delta w\, dS - \int_\Gamma \delta\psi\int_o^t p_n^0 dt\, dS\Big)dt, \quad (13)$$

This variational form, which must hold for arbitrary δv, δw and $\delta\psi$, will be the basis for the discretization process. In our approximate procedure, the exact absorbing boundary condition which appears in the last term on the left side of (13), will be replaced by the approximate set of Eqs. (10). (The implementation of the alternative conditions (9*a*) and (9*b*) is straightforward.) To introduce these equations into the variational form (13) it suffices to replace the term that contains the exact value $\mathfrak{F}$ of the normal derivative of ψ by its approximate counterpart and integrate the terms containing second derivatives by parts. There results:

$$-\int_{\Gamma_a}\mathfrak{F}[\psi]\delta\psi dS_a = \int_{\Gamma_a}\left(\frac{1}{c}\dot\psi + \frac{1}{R}\psi\right)\delta\psi dS_a$$
$$+\int_{\Gamma_a}\frac{c}{2\gamma R^2}(1-\eta^2)\psi_\eta^{(1)}\delta\psi_\eta dS_a$$
$$+\int_{\Gamma_a}\frac{c}{2\gamma R^2}(1-\eta^2)\left[\psi_\eta - \psi_\eta^{(1)} - \frac{1}{\gamma}\dot\psi_\eta^{(1)}\right]\delta\psi_\eta^{(1)}dS_a, \quad (14)$$

where dS_a above is equal to $-R^2 d\eta$. It is important to observe that with the replacement (14) the variational operator in (13) will lead, upon spatial discretization, to a symmetric system of ordinary differential equations.

3 Finite Element Discretization

The spatial discretization of (13) with the replacement shown in (14) involves using standard finite element piecewise polynomial approximations for the displacements v and w on Γ, the velocity potential ψ in the closure $\bar\Omega^f$ of Ω^f, and the auxiliary function $\psi^{(1)}$ on Γ_a, as follows:

$$v(\mathbf{x},t) = \boldsymbol{\alpha}^T(\mathbf{x})\mathbf{v}(t), \quad w(\mathbf{x},t) = \boldsymbol{\alpha}^T(\mathbf{x})\mathbf{w}(t),$$
$$\psi(\mathbf{x},t) = \boldsymbol{\beta}^T(\mathbf{x})\boldsymbol{\psi}(t), \quad \psi_\eta^{(1)}(\mathbf{x},t) = \boldsymbol{\sigma}^T(\mathbf{x})\boldsymbol{\zeta}(t), \quad (15)$$

in which, $\boldsymbol{\alpha}$, $\boldsymbol{\beta}$ and $\boldsymbol{\sigma}$ are vectors of global shape functions; $\mathbf{v}$, $\mathbf{w}$, $\boldsymbol{\psi}$ and $\boldsymbol{\zeta}$ are the unknown nodal displacements, potential velocities, and auxiliary functions, defined over Γ, Ω^f, and Γ_a, initially at rest. The global shape functions $\boldsymbol{\alpha}(\mathbf{x})$ have continuous first derivatives on Γ; $\boldsymbol{\beta}(\mathbf{x})$ is continuous over $\bar\Omega^f$, and $\boldsymbol{\sigma}(\mathbf{x})$ is continuous over Γ_a. Notice that we approximate $\psi_\eta^{(1)}$ rather than $\psi^{(1)}$ directly, in order to avoid singular matrices in later calculations. The corresponding virtual quantities $\delta v(\mathbf{x})$, $\delta w(\mathbf{x})$, $\delta\psi(\mathbf{x})$, and $\delta\psi_\eta^{(1)}(\mathbf{x})$ are approximated by the same global functions as their respective trial functions. After substituting (15) and the corresponding virtual quantities into (13) with (14), and noting that $\boldsymbol{\delta}\mathbf{v}$, $\boldsymbol{\delta}\mathbf{w}$, $\boldsymbol{\delta\psi}$ and $\boldsymbol{\delta\zeta}$ are arbitrary, there results a system of ordinary differential equations with the following structure:

$$M\ddot{\mathbf{U}} + C\dot{\mathbf{U}} + K\mathbf{U} = \mathbf{F}, \quad (16)$$

where $\mathbf{U}^T = ([\mathbf{v}^T, \mathbf{w}^T], [\boldsymbol{\psi}_\Gamma^T, \boldsymbol{\psi}_{\Omega^f}^T], [\boldsymbol{\psi}_{\Gamma_a}^T, \boldsymbol{\zeta}^T])$ and $\boldsymbol{\Gamma}_\Gamma$, $\boldsymbol{\psi}_{\Omega f}$ and $\boldsymbol{\psi}_{\Gamma_a}$ denote partitions of ψ over Γ, Ω^f, and γ_a, respectively; M, C, and K are the mass, damping, and stiffness matrices of the system, and $\mathbf{F}(t)$ represents the effective wave excitation.

The matrices M, C, and K have the form:

$$M = \begin{bmatrix} M^s & 0 & 0 \\ 0 & M^f & M^f_{\psi_{\Omega f}\psi_{\Gamma_a}} \\ 0 & M^f_{\psi_{\Gamma_a}\psi_{\Omega f}} & M^f_{\psi_{\Gamma_a}\psi_{\Gamma_a}} \end{bmatrix},$$

$$C = \begin{bmatrix} 0 & C^{sf}_{w\psi_\Gamma} & 0 \\ C^{fs}_{\psi_\Gamma w} & 0 & 0 \\ 0 & 0 & C^a \end{bmatrix},$$

$$K = \begin{bmatrix} M^s & 0 & 0 \\ 0 & K^f & K^f_{\psi_{\Omega f}\psi_{\Gamma_a}} \\ 0 & K^f_{\psi_{\Gamma_a}\psi_{\Omega f}} & K^f_{\psi_{\Gamma_a}\psi_{\Gamma_a}} + K^a \end{bmatrix} \quad (17a,b,c)$$

The matrices M and K consist of three sets of block-diagonal matrices, each representing a different part of the system. The individual matrices within each block are designated by the superscripts s, f, or a, to indicate explicitly that they correspond to the structure (shell), the fluid, or the absorbing boundary. Thus, the top left blocks are the standard mass and stiffness matrices associated with the shell, the middle blocks contain the corresponding sets for the fluid, and the bottom right block in (17*b*) and (17*c*) represents the effective damping and stiffness of the absorbing boundary.

Notice that the only coupling in the K matrix occurs between the fluid and the absorbing boundary. The shell and the fluid are coupled only through submatrices $C^{sf}_{w\psi_\Gamma}$ and $C^{fs}_{\psi_\Gamma w}$ of the matrix C. Even though these submatrices operate on the first time derivative of U there is no energy dissipation associated with them since the idealized structure has been taken to be undamped and the fluid is inviscid. The only damping in the actual, unbounded, system comes from the radiated energy, which, in our formulation, is modeled through the bottom right block of C associated with the absorbing boundary.

From Eqs. (14) and (17) it is seen that the absorbing boundary is characterized completely by the damping and stiffness matrices C^a and K^a, defined by:

$$C^a = \begin{bmatrix} C^a_{\psi_{\Gamma_a}\psi_{\Gamma_a}} & 0 \\ 0 & C^a_{\eta\eta} \end{bmatrix}, \quad K^a = \begin{bmatrix} K^a_{\psi_{\Gamma_a}\psi_{\Gamma_a}} & K^a_{\psi_{\Gamma_a}\zeta} \\ K^a_{\zeta\psi_{\Gamma_a}} & K^a_{\zeta\zeta} \end{bmatrix}, \quad (18)$$

as there is no inertia associated with our approximate absorbing boundary. Since C^a and K^a are local and symmetric they can be constructed element by element and incorporated into the equations of motion by standard assembly techniques using existing finite element software. All that is necessary is to incorporate the element matrices c^a and k^a corresponding to the global C^a and K^a into the finite element library of an existing software package for interior problems. The same finite element software package can then be used to solve the complete system of Eqs. (16), in either assembled form, node-by-node, or element-by-element, by means of its own step-by-step time integrator. To illustrate that the element matrices c^a and k^a that characterize the absorbing, or impedance, element have, indeed, a simple form, we provide below the corresponding element matrices for the particular case of the spherical absorbing boundary with the choice of $\gamma = c/R$:

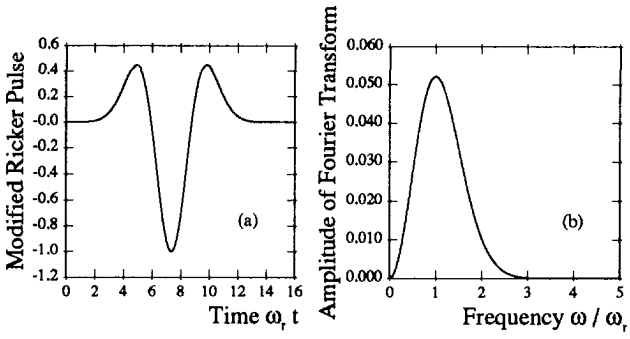

Fig. 2 (*a*) Finite-duration modified Ricker pulse; (*b*) amplitude of Fourier Transform of (a)

$$K^a = R\begin{bmatrix} \int_{\Gamma_a^e} \boldsymbol{\beta}\boldsymbol{\beta}^T d\eta & \frac{1}{2}\int_{\Gamma_a^e}(1-\eta^2)\boldsymbol{\beta}_\eta \boldsymbol{\sigma}^T d\eta \\ \frac{1}{2}\int_{\Gamma_a^e}(1-\eta^2)\boldsymbol{\sigma}\boldsymbol{\beta}_\eta^T d\eta & -\frac{1}{2}\int_{\Gamma_a^e}(1-\eta^2)\boldsymbol{\sigma}\boldsymbol{\sigma}^T d\eta \end{bmatrix}, \tag{19a}$$

$$c^a = \frac{R^2}{c}\begin{bmatrix} \int_{\Gamma_a^e} \boldsymbol{\beta}\boldsymbol{\beta}^T d\eta & 0 \\ 0 & -\frac{1}{2}\int_{\Gamma_a^e}(1-\eta^2)\boldsymbol{\sigma}\boldsymbol{\sigma}^T d\eta \end{bmatrix}, \tag{19b}$$

where the integration is over an element Γ_a^e of Γ_a.

We complete our description of the finite element discretization by giving some details about the forcing function **F** in (16). From (13) it is clear that **F** has non-zero values only for the degrees of freedom associated with the nodal shell radial displacements and the fluid velocity potential, i.e., $\mathbf{F}^T = ([0^T, \mathbf{F}_w^T], [\mathbf{F}_{\psi\Gamma}^T, 0^T], [0^T, 0^T])$, where:

$$\mathbf{F}_w(t) = \int_\Gamma p^0 \boldsymbol{\alpha} dS, \quad \mathbf{F}_{\psi\Gamma}(t) = -\int_\Gamma \int_0^t p_n^0 dt \boldsymbol{\beta} dS. \quad (20a,b)$$

We recall that for the scattering problem discussed thus far p^0 and p_n^0 are the pressure and the normal derivative of the pressure of the prescribed incident wave on the wet surface Γ. If one is interested in the radiation problem, one need only interpret p^0 in (20*a*) as the normal pressure applied directly on the shell and set $\mathbf{F}_{\psi\Gamma}$ equal to zero.

Clearly, (16) can be solved by standard step-by-step integration schemes; in this paper the numerical results are obtained by the trapezoidal rule. It also can readily be solved as an algebraic system in the case of a time-harmonic steady-state excitation $\mathbf{F} = \bar{\mathbf{F}}e^{i\omega t}$.

4 Numerical Examples

The numerical experiments aim primarily at assessing the accuracy and validity of the suggested methodology with particular focus on the performance of the impedance element (IE) (corresponding to the implementation of conditions (10)) in the transient regime. To this end simple canonical systems are considered in two specific conditions. One corresponds to a spherical homogeneous elastic shell submerged in water and the other to the limiting rigid case. The relative properties for the homogeneous shell are:

$$c_s/c = 3.53,\ \rho_s/\rho = 7.65,\ \nu = 0.3, \text{ and } d/a = 0.01.$$

In both cases we consider a traveling plane wave that impinges upon the shell (scattering problem) as the exterior excitation, i.e. $p^0(\mathbf{x}, t) = P^0 f(\omega_r[t + (r\cos\phi - R)/c])$, where

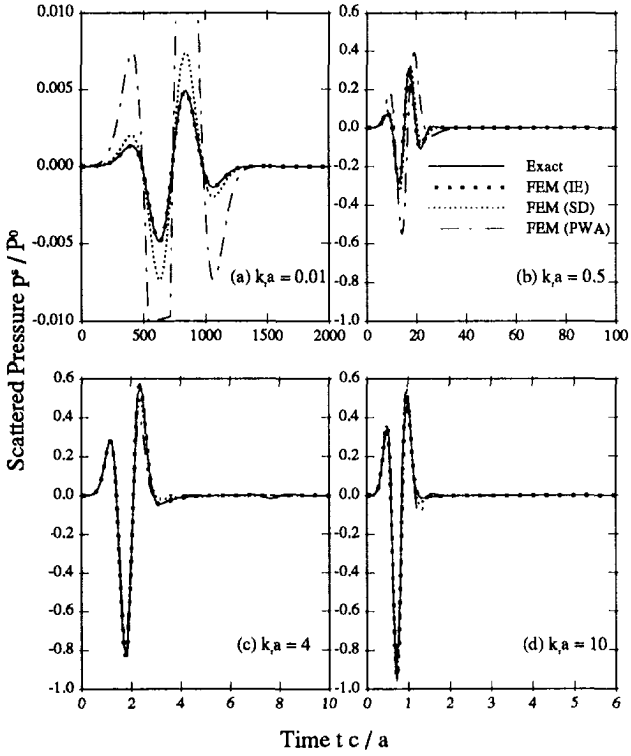

Fig. 3 Backscattered pressure directly on a rigid scatterer, exact and FEM solutions; absorbing boundary at $r/a = 1.2$; (*a*) $n_r = 2$, $n_\phi = 8$, (*b*) $n_r = 2$, $n_\phi = 8$, (*c*) $n_r = 2$, $n_\phi = 32$, (*d*) $n_r = 4$, $n_\phi = 64$

P^0 is a constant and f is the time signal represented by a finite-duration modified Ricker (1977) pulse of unit amplitude as shown in Fig. 2(*a*) for the point of incidence ($r = R$, $\phi = 0$); ω_r is the dominant frequency of the excitation. The amplitude of the corresponding Fourier transform is shown in Fig. 2(*b*). The numerical results in this section were obtained by using piecewise cubic Hermite polynomials for the shell, eight-noded quadratic elements for the fluid, and three-noded quadratic elements with two degrees of freedom per node for the boundary elements. In all cases the incident wave propagates from east to west. All the calculations were carried out with a time step of $c\Delta t/a = 0.1$.

Figure 3 depicts the normalized backscattered pressure directly on a rigid spherical scatterer as a function of normalized time, for different values of the dimensionless wave number $k_r a$, where $k_r = \omega_r/c$ is the dominant wave number of the Ricker pulse. Notice the different horizontal and vertical scales for the various wave numbers. The dotted and stippled lines represent the numerical solutions (FE) of the problem when the spherical absorbing boundary is placed at a distance $r/a = 1.2$ from the center of the scatterer, i.e., at only $0.2a$ from the wet surface of the scatterer. (The number of radial and angular elements, n_r and n_ϕ, used for each wave number are indicated in the figure caption.) These solutions are to be compared against the corresponding exact solutions, shown by solid lines, obtained by inversion via FFT of the exact frequency-domain solution of the original exterior problem. The lighter dotted line and the stippled line correspond to the implementation of conditions (9*a*) and (9*b*), respectively, as the absorbing boundary. Mechanically (9*b*) is analogous to a spring and a dashpot in parallel, hence the SD designation in the figure, while condition (9*a*) is the widely used PWA boundary. It can be seen that the darker dotted line which corresponds to the IE element is practically indistinguishable from the exact curve for all low- (Fig. 3*a*, *b*) and high-frequency (Fig. 3*c*, *d*) pulses; errors exhibited by the use of SD and PWA boundaries for the low-frequency

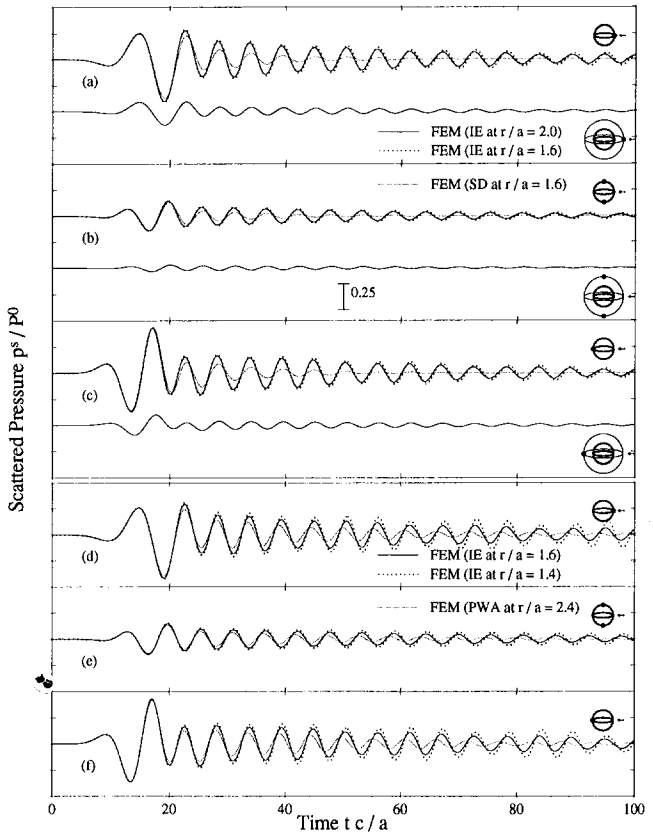

Fig. 4 Scattered pressure at various points (denoted by solid bullets) for different boundaries, on and near a shell due to an incident plane wave; $n_r = 4$ $(r/a = 1.4)$, $n_r = 6$ $(r/a = 1.6)$, $n_r = 10$ $(r/a = 2)$, $n_r = 14$ $(r/a = 2.4)$, $n_\phi = 32$, $k_r a = 0.5$

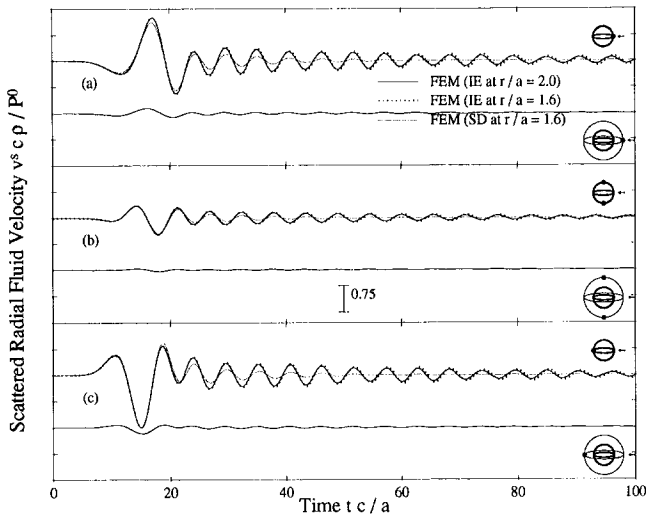

Fig. 5 Scattered radial fluid velocity at various points (denoted by solid bullets) for different boundaries, on and near a shell due to an incident plane wave; $n_r = 6$ $(r/a = 1.6)$, $n_r = 10$ $(r/a = 2)$, $n_\phi = 32$, $k_r a = 0.5$

pulses are unacceptable while their accuracy improves dramatically as the dominant wave number of the pulse is increased.

Next we consider the response of a homogeneous shell to an incident plane wave for a dominant wavenumber $k_r a = 0.5$. Figure 4 shows the normalized scattered pressure computed at different points on the wet surface of the shell and within the fluid on the absorbing boundary. (The points are identified by solid bullets in the inserts shown in the figure.) There are three curves in each of Figs. 4 to illustrate the effect of using different boundary conditions/elements at various locations on the scattered pressure. The top set of figures (Figs. 4*a*, *b*, *c*) depict results corresponding to placing the impedance element (IE) at $r/a = 1.6$ (dark dotted line) and at $r/a = 2$ (solid line), and the SD boundary at $r/a = 1.6$ (light dotted line). The two IE curves are very close; increasing the distance from the shell further results in practically indistinguishable curves. Hence we regard the IE curve with $r/a = 2$ as the exact solution. On the other hand, results obtained with the SD boundary produce a clear overdamping. This is at variance with the accurate behavior exhibited by the SD element on Fig. 3 for the rigid scatterer. This difference in performance is caused by the significant participation of the higher modes of the shell on the response, which gives rise to more rapid oscillations of the scattered pressure around the deformable scatterer. Figures 4*d*, *e*, *f* depict solutions corresponding to the IE located at $r/a = 1.4$ (dark dotted line) and $r/a = 1.6$ (solid line) and to the plane wave approximation PWA at $r/a = 2.4$ (light dotted line). Using the results for the IE at $r/a = 1.6$ as reference it is clear that moving the IE too close to the shell results in increasing errors. The traces for the PWA boundary indicate that the error for this boundary can be significant even when it is placed at a considerable distance from the shell. Figure 4 demonstrates, in brief, that the new IE element provides the highest degree of accuracy among the three types of elements considered herein; the SD element is next, followed by the PWA element, consistent with the predicted asymptotic behavior of the approximations (10*a*, *b*), (9*b*), and (9*a*). Clearly, any desired accuracy can be attained with the SD and PWA elements provided they are placed sufficiently far from the scatterer. This, of course, results in larger buffer zones, and thus, in less efficient calculations.

To illustrate the effect of the shell on the velocity of the fluid in the vicinity of the shell, Fig. 5 shows the scattered radial fluid velocity at various locations. The pattern is similar to that of the scattered pressure, with the velocity of the outgoing, evanescent, waves decaying even faster than the corresponding scattered pressure.

5 Concluding Remarks

One of the major objectives of this paper was to assess the overall merits of the proposed methodology. In light of the excellent agreement between the approximate and exact solutions obtained for the test problems as well as the significant economy achieved, it appears that the new methodology based on finite element spatial discretization, standard step-by-step time integration, and a novel impedance element, provides a practical and accurate means for solving complex problems in structural acoustics involving axisymmetric structures in either the time or the frequency domain. The methodology can be applied directly to arbitrary three-dimensional axisymmetric elastic structures merely by using the appropriate expression in (12) for the kinetic and strain energy of the submerged structure.

The novel impedance element permits one to retain the familiar form of the discretized equations of motion for the structure with their sparsity and symmetry intact. Since the element is completely represented by a pair of local symmetric stiffness and damping matrices, the entire procedure lends itself to easy incorporation into existing finite element codes for interior problems. It also allows for ready parallelization that will best exploit the main features of particular advanced architectures.

Acknowledgment

The work of L. F. Kallivokas was supported by Swanson Analysis Systems, Inc. We are grateful for this support. We also thank the reviewers for their helpful suggestions.

References

Barry, A., Bielak, J., and MacCamy, R. C., 1988, "On Absorbing Boundary Conditions for Wave Propagation," *J. Comput. Phys.*, Vol. 79, pp. 449–468.

Bayliss, A., and Turkel, E., 1980, "Radiation Boundary Conditions for Wave-Like Equations," *Comm. Pure Appl. Math.*, Vol. 33, No. 6, pp. 707–725.

Chertock, G., 1970, "Transient Flexural Vibrations of Ship-Like Structures Exposed to Underwater Explosion," *J. Acoust. Soc. Am.*, Vol. 48, No. 1, pp. 170–180.

Engquist, B., and Majda, A., 1979, "Radiation Boundary Conditions for Acoustic and Elastic Wave Calculations," *Comm. Pure Appl. Math.*, Vol. 32, No. 3, pp. 313–357.

Everstine, G. C., 1981, "A Symmetric Potential Formulation for Fluid-Structure Interaction," *J. Sound and Vib.*, Vol. 79, No. 1, pp. 157–160.

Geers, T. L., 1971, "Residual Potential and Approximate Methods for Three-Dimensional Fluid-Structure Interaction Problems," *J. Acoust. Soc. Am.*, Vol. 49, No. 5, pp. 1505–1510.

Geers, T. L., 1978, "Doubly Asymptotic Approximation for Transient Motions of Submerged Structures," *J. Acoust. Soc. Am.*, Vol. 64, No. 5, pp. 1500–1508.

Givoli, D., 1991, "Non-reflecting Boundary Conditions: A Review," *J. Comput. Phys.*, Vol. 94, No. 1, pp. 1–29.

Jeans, R. A., and Mathews, I. C., 1990, "Solution of Fluid-Structure Interaction Problems Using a Coupled Finite Element and Variational Boundary Element Technique," *J. Acoust. Soc. Am.*, Vol. 88, No. 5, pp. 2459–2466.

Junger, M. C., and Feit, D., 1972, *Sound, Structures, and Their Interaction*, MIT Press, Cambridge, MA.

Kallivokas, L. F., Bielak, J., and MacCamy, R. C., 1991, "Symmetric Local Absorbing Boundaries in Time and Space," *J. Eng. Mech.*, Vol. 117, No. 9, pp. 2027–2048.

Kallivokas, L. F., and Bielak, J., 1993, "Time-Domain Analysis of Transient Structural Acoustics Problems Based on the FEM and a Novel Absorbing Boundary Element," *J. Acoust. Soc. Am.*, Vol. 94, No. 6, pp. 3480–3492.

Mindlin, R. D., and Bleich, H. H., 1953, "Response of an Elastic Cylindrical Shell to a Transverse, Step Shock Wave," *J. Appl. Mech.*, Vol. 20, pp. 189–195.

Pinsky, P. M., Thompson, L. L., and Abboud, N. N., 1992, "Local High-Order Radiation Boundary Conditions for the Two-Dimensional Time-Dependent Structural Acoustics Problem," *J. Acoust. Soc. Am.*, Vol. 91, No. 3, pp. 1320–1335.

Pinsky, P. M., and Abboud, N. N., 1990, "Transient Finite Element Analysis of the Exterior Structural Acoustics Problem," ASME JOURNAL OF VIBRATIONS AND ACOUSTICS, Vol. 112, pp. 245–256.

Pinsky, P. M., and Abboud, N. N., 1991, "Finite Element Solution of the Transient Exterior Structural Acoustics Problem Based on the Use of Radially Asymptotic Boundary Operators," *Comput. Methods Appl. Mech. Eng.*, Vol. 85, pp. 311–348.

Ricker, N. H., 1977, *Transient Waves in Visco-Elastic Media*, Elsevier Scientific Publishing Company, Amsterdam, Netherlands.